Large-Scale Dynamic Spectrum Access with IEEE 1900.5.2 Spectrum Consumption Models

Prasad Netalkar*, Azhaan Zahabee†, Carlos E. Caicedo Bastidas‡, Igor Kadota†, Dragoslav Stojadinovic*, Gil Zussman†, Ivan Seskar*, Dipankar Raychaudhuri*

*WINLAB, Rutgers University, USA †Columbia University, USA ‡Syracuse University, USA

*{pnetalka, stojadin, seskar, ray}@winlab.rutgers.edu †{azhaan.z, igor.kadota, gil.zussman}@columbia.edu ‡ccaicedo@syr.edu

***Abstract*—Next generation wireless services and applications, including Augmented Reality, Internet-of-Things, and Smart-Cities, will increasingly rely on Dynamic Spectrum Access (DSA) methods that can manage spectrum resources rapidly and efficiently. Advances in regulatory policies, standardization, networking, and wireless technology are enabling DSA methods on a more granular basis in terms of time, frequency, and geographical location which are key for the operation of 5G and beyond-5G networks. In this context, this paper proposes a novel DSA algorithm that leverages IEEE 1900.5.2 Spectrum Consumption Models (SCMs) which offer a mechanism for RF devices to: (i) "announce" or "declare" their intention to use the spectrum and their needs in terms of interference protection; and (ii) determine compatibility (i.e., non-interference) with existing devices. In this paper, we develop an SCM-based DSA algorithm for spectrum deconfliction in large-scale wireless network environments and evaluate this algorithm in terms of computation time, efficiency of spectrum allocation, and number of device reconfigurations due to interference using a custom simulation platform. The results demonstrate the benefits of using SCMs and their capabilities to perform fine grained spectrum assignments in dynamic and dense communication environments.**

***Index Terms*—Dynamic spectrum access, Spectrum sharing, Spectrum consumption models, Wireless networks, 5G**

I. Introduction

The evolution of wireless communication services and technologies increasingly relies on enhanced algorithms for spectrum management that enable heterogeneous devices to share limited spectrum resources and coexist harmoniously. Various DSA methods have been proposed and evaluated in the literature. In [1], the authors present an in-depth survey on recent Spectrum Sharing (SS) techniques that use DSA, categorizing them in terms of their architecture (i.e., centralized or distributed), spectrum allocation behavior (i.e., cooperative or non-cooperative), and method (i.e., dynamic exclusive, open access, and hierarchical). The survey discussed various SS techniques which uses concepts from game theory, information theory, stochastic modeling, and several database assisted algorithms. Yet, there are still many open problems in SS related to real implementation, standardization, privacy, and system architectural design.

In [2], the authors proposed SMAP, a policy-driven distributed spectrum management architecture which uses an aggregated radio map to exchange spectrum information among peers for spectrum assignment. The authors of [2] didn't provide details on the syntax and schematics of the radio map and their evaluation was restricted to a small topology in which nodes were only allowed to adjust their frequencies. Authors in [3], [4] presented a Radio Environment Map (REM) based spectrum access architecture to protect primary incumbents and share the available spectrum. The REMs are constructed from sensor measurements and are used to determine the channel availability and also to estimate interference levels at each location of interest. The architecture is based on centralised storage databases and the methods to determine compatibility among incumbents and secondary users are not standardised. These methods depend on the tools used to perform spectrum use/occupancy analysis and their results are often debatable by each of parties involved [5].

Motivated by DARPA's efforts on the Spectrum Collaboration Challenge (SC2) and also ongoing standardization by the IEEE [6], in this work we develop a novel algorithm to perform large-scale DSA operations in wireless environments using Spectrum Consumption Models (SCMs). SCMs offer a standardized mechanism [7] for RF devices to "announce" or "declare" their intention to use the spectrum (in the case of transmitters) or their needs in terms of spectrum protection (in the case of receivers and passive devices). This declaration (i.e., the SCM) can simplify spectrum use coordination when compared to DSA algorithms that rely solely on sensing to avoid interference between several RF transmitters and receivers [8], [9]. In our previous work [10], we built a simple spectrum access framework on the NSF PAWR COSMOS testbed [11] that performed DSA coordination automatically using SCMs that expressed the intended spectrum use and interference protections needed for three different wireless networks. In this paper, we develop a novel ***SCM-based Spectrum Deconfliction (SD) algorithm*** that takes into consideration aggregate interference and makes use of frequency and power adjustments to deconflict spectrum use. We built a custom simulation framework to evaluate the algorithm's performance, scalability and feasiblity of SCM-based DSA for coordinating spectrum use in dynamic and dense communication environments.

The remainder of this paper is organised as follows. Section II introduces SCMs. Section III provides a brief description of how SCMs are used to deconflict spectrum assignments (i.e. the compatibility computation). In Section IV, we develop the SCM-based DSA algorithm. Section V describes the simulation platform developed to evaluate SCM-based DSA algorithms and discusses simulation results from the proposed algorithm. Section VI concludes the paper and discusses future work.

II. SCM - Background

SCMs use a set of 11 data elements, referred to as constructs, to describe the spectral, spatial, and temporal characteristics of spectrum use by any RF device and/or system. These constructs, which are defined in the IEEE 1900.5.2 standard [7], [12], can be used to build different types of SCMs, including: (i) ***Transmitter models*** that convey the extent and strength of RF emissions from a transmitter; (ii) ***Receiver models*** that convey what harmful interference to an RF receiver device is; and (iii) ***System and Set models*** that group several transmitter and receiver SCMs. The SCM constructs most relevant to this work are described below. Unless otherwise stated, the constructs must be used in both transmitter and receiver models.

- ***Reference Power:*** Value that provides a reference power level for the emission of a transmitter or for the allowed interference in a receiver. It is used as the reference power value for the spectrum mask, underlay mask, and power map constructs.
- ***Spectrum mask:*** Defines the relative spectral power density of emissions by frequency. This construct is mandatory for Transmitter models only (see Fig. 1(a)).
- ***Underlay mask:*** Defines the relative spectral power density of allowed interference by frequency. This construct is mandatory for Receiver models only (see Fig. 1(b)).
- ***Power map:*** Defines a relative power flux density per solid angle. It conveys the dispersion of electromagnetic energy from a transmitter's antenna or the concentration of energy at a receiver antenna.
- ***Propagation map:*** Defines a path loss model per solid angle.
- ***Schedule:*** Specifies the time in which the model applies (start time, end time). Periodic activity can also be defined.
- ***Location:*** Specifies where an RF device may be used.

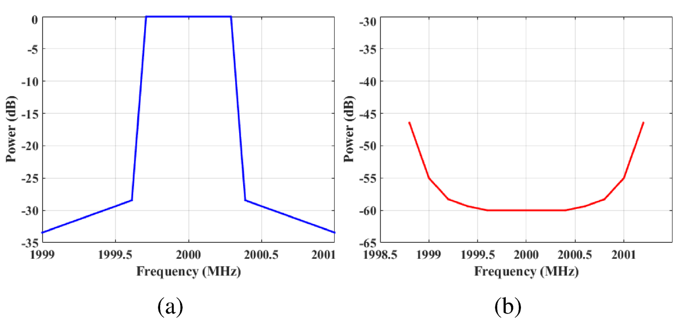

Fig. 1: (a) Tx spectrum mask. (b) Rx underlay mask.

Additional SCM constructs can be used to describe intermodulation effects, policy or protocol based spectrum coexistence, and broadcasting behavior. Using the information provided by the SCMs, any entity can use the methods standardized in IEEE 1900.5.2 to evaluate whether the spectrum use of two or more Spectrum Dependent Systems (SDSs) is compatible. The compatibility test indicates whether the SDSs can coexist without causing harmful interference to each other (i.e., they are compatible SDSs) or if they will interfere with each other (i.e., they are non-compatible SDSs). This computation can be extended to scenarios with multiple devices where aggregate interference effects need to be taken into account and which can be used as part of any compatibility decision.

III. DSA with SCMs

A. Compatibility test for a transmitter-receiver pair

The Compatibility Test (CT) using SCMs aims at determining if a transmitter model is compatible with a receiver model. CT begins by checking if the SCMs overlap in both time and frequency. If they do not overlap, there is compatibility. If they do overlap, then the evaluation continues. The IEEE 1900.5.2 standard describes how to compute the power spectral flux density (PSFD) from the transmitter at the location of the receiver and the corresponding maximum allowed interference power for the receiver. In case the transmitter does not exceed the receiver's maximum allowed interference power, the devices are declared compatible. The difference between the maximum allowed interference and the transmitter's power at the receiver's location is the *power margin*. The power margin can be used to determine by how much a transmitter's power could be increased – if necessary (e.g., to expand coverage) – while still being compatible with the receiver. Alternatively, in case the devices are declared incompatible, the power margin can be used to determine the amount of attenuation necessary at the transmitter to achieve compatibility [12].

B. Compatibility test for multiple devices

When several transmitters and receivers interfere with one another, the CT is based on the computation of the *aggregate interference* caused by the transmitters under consideration at a particular receiver. Aggregate compatibility is achieved when the aggregate interference at every receiver under consideration is below its maximum allowable interference power [12]. The IEEE 1900.5.2 standard provides guidelines and a method to compute aggregate compatibility, using SCMs, for scenarios with many receiver and transmitter devices. When the locations of transmitters and receivers are static, the compatibility test for a single transmitter-receiver (Tx/Rx) pair can be easily extended to the multiple transmitters and multiple receivers case. When there is mobility, before evaluating compatibility, the most constraining configuration for a particular receiver needs to be found. This configuration should be a feasible positioning and configuration of all devices in the scenario that maximizes the aggregate interference on that receiver [12], [13]. In this work, we focus on static devices. Mobility related issues are left for future work.

IV. Algorithm for Large-Scale DSA

In this section, we develop an enhanced SCM-based DSA algorithm that can deconflict the spectrum use of networks with a large number of RF devices. The algorithm leverages SCMs in a series of spectrum use compatibility computations and message exchanges to dynamically determine the transmission parameters of devices, in particular their central frequency and transmission power levels, in order to achieve *aggregate* *compatibility*. Each network composed of a single transmitter-receiver pair has a designated wireless domain (WD) controller, which can interact with other WD controllers. For the exchange of SCM-based messages between WD controllers, a modified version of the Collaborative Interaction Language (CIL) [10] developed for DARPA SC2 can be leveraged to enable information exchange. To evaluate the performance of this algorithm, we use a custom-made simulation platform described in Sec. V.

Our SCM-based Spectrum Deconfliction (SD) method is described in Algorithm 1 with key terms defined in Table I. When a new pair of devices (Tx$_n$ and Rx$_n$) enters an operational area, the SD algorithm running at the corresponding WD controller requests the SCMs of new and existing Tx and Rx pairs and then it initializes the following parameters: compatibility score ($ct\_score = 0$), total power margin ($total_{PM} = 0$), and maximum power margin ($max_{PM} = 0$). The score is increased every time a new Tx or Rx under evaluation is determined to be compatible with a pre-existing RF counterpart (Tx vs. Rx, or, Rx vs. Tx) and is used to verify the compatibility of a new Tx/Rx pair with the entire system whereas the power margins are used to verify whether small adjustments in the power level of the new transmitter (Tx$_n$) can make it compatible with existing receivers.

As the WD controller performs CTs between the new Rx$_n$ and existing transmitters (Tx$_1$,...,Tx$_{n-1}$), if there is compatibility, the WD controller computes and updates the total aggregate interference ($total_{TP}$) at Rx$_n$. With the total aggregate interference value an aggregate evaluation of compatibility is performed. If Rx$_n$ is not compatible with the existing transmitters, i.e., if the $total_{TP}$ is greater than the allowable interference power at Rx$_n$ (identified as $P_{allowRx_n}$), the Tx/Rx pair is moved to a different frequency channel and the CTs start over. More details on the frequency assignment scheme will be discussed later. On the other hand, if Rx$_n$ is compatible with the existing transmitters, the WD controller verifies whether Tx$_n$ is compatible with the existing receivers (Rx$_1$,...,Rx$_{n-1}$). To that end, it computes the interference caused by Tx$_n$ at the existing receivers and compares it with max_{PM}. If Tx$_n$ is compatible with the existing receivers, the WD controller sets up the new link and updates the contribution of this new transmitter to the aggregate interference seen by each receiver using the matrix (Rx_{interf}). Otherwise, the WD controller attempts to achieve compatibility by decreasing Tx$_n$'s power by no more than the value of a previously agreed upon power margin threshold ($power_{MT}$). In case the power adjustment fails to achieve compatibility, the WD controller chooses a different frequency channel for the Tx/Rx pair and the CTs start over. At the end of the algorithm, once aggregate compatibility is achieved, the WD controller sets up the link and updates the SCMs of Tx$_n$ and Rx$_n$ based on the frequency and power values found to achieve global (scenario wide) compatibility so that they are ready for future CTs.

Algorithm 1 Spectrum Deconfliction (SD) involving aggregate interference, frequency, and power adjustments

Input: SCMs of new and existing Tx/Rx pairs
Output: Deconflicted Tx/Rx pairs
Initialize: $power_{MT}$ and $Rx_{interf} = [\ ]$
for *every new set of Tx/Rx pair* **do**
  WD_n controller collects Tx/Rx SCMs
  Initialize: $ct\_score = 0$, $total_{TP} = 0$ and $max_{PM} = 0$
  for *Rx$_n$ perform CT between* $Tx_1..Tx_i..Tx_{n-1}$ **do**
    $total_{TP} = total_{TP} + P_{in}$
    if *compatible* **then**
      $ct\_score = ct\_score + 1$
  if $ct\_score == n-1$ ***and*** $total_{TP} \leq P_{allowRx_n}$ **then**
    Initialize: $ct\_score = 0$ and $Rx_{interf\_n} = [\ ]$
    $Rx_{interf}[n] = total_{TP}$
    for *Tx$_n$ perform CT between* $Rx_1..Rx_j..Rx_{n-1}$ **do**
      $Rx_{interf\_n}[j] = P_{nj}$
      $curr_{PM} = Rx_{interf}[j] + P_{nj} - P_{allowRx_j}$
      $max_{PM} = max(max_{PM}, curr_{PM})$
      if *compatible* ***and*** $current_{PM} \leq 0$ **then**
        $ct\_score = ct\_score + 1$
    if $ct\_score == n-1$ **then**
      $Rx_{interf} = Rx_{interf} + Rx_{interf\_n}$
    else if $max_{PM} \leq power_{MT}$ **then**
      Adjust Tx$_n$ reference power based on max_{PM}
      Update Rx_{interf} based on max_{PM} and Rx_{interf_n}
      Verify if the new link is reachable or not
      if *link* ***not*** *reachable* **then**
        Change Rx$_n$ and Tx$_n$ frequency and recompute CTs
    else
      Change Rx$_n$ and Tx$_n$ frequency and recompute CTs
  else
    if $total_{TP} > P_{allowRx_n}$ ***and*** $ct\_score == n-1$ **then**
      Aggregate interference detected
    Change Rx$_n$ and Tx$_n$ frequency and recompute CTs
  Update Rx$_n$ and Tx$_n$ SCM and setup the link

Regarding frequency assignment: Upon entering the operational area, all RF devices start with a default center frequency f_c and, if needed, they move to new frequencies in Δf increments until a compatible frequency for the operation of the new Tx/Rx pair is found. The objective here is to achieve high spectrum efficiency by minimizing the number of different frequency channels used. Thus, other approaches to determining f_c and Δf can be used, but they are left for future research.

TABLE I: Key Parameters of Algorithm 1

Parameter	Description
P_{ij}	Interference power at jth RX from ith TX
Rx_{interf}	Interference at each RX from all existing TXs
Rx_{interf_n}	Interference at each RX from TX$_n$
$total_{TP}$	Total power at RX$_n$ from all existing TXs
$power_{MT}$	Power margin threshold (PMT)
max_{PM}	Max power margin from all RXs
$curr_{PM}$	Current power margin
$P_{allowRx_n}$	Allowable power at RX$_n$

V. Simulation Analysis and Results

To evaluate the performance of our proposed SD algorithm, we use a Python-based simulator that assigns Tx/Rx pairs to random locations on a given operational area and then uses Algorithm 1 to deconflict spectrum use. The simulation uses an event-based framework with Tx/Rx pairs joining the system sequentially, i.e., one after the other. The simulation parameters are summarized in Table II. To perform CTs, we leverage Octave code from the Spectrum Consumption Model Builder and Analysis Tool (SCMBAT) [14] which interfaces with our python simulator using *oct2py*.

The SCMs used in the simulator are similar to the SCMs from our experimental work in [10], except that, now we are limiting the transmit power such that the coverage radius for each Tx is around 100 meters. The structure of the transmitter spectrum mask and the receiver underlay mask used are illustrated in Fig. 1. The positions of the transmitters are chosen uniformly at random in a 0.5 square mile area, subject to the constraint of a minimum distance of 10 meters between any two transmitters. Moreover, the separation between a transmitter and the associated receiver is chosen uniformly at random in the interval between 10 and 100 meters. Next, for a scenario involving a large number of RF devices, we discuss the simulation results for the spectrum deconfliction performance of Algorithm 1 against the baseline algorithm [10] that only adjusts center frequencies to deconflict spectrum use, in terms of its spectrum resource usage and computation time.

TABLE II: Simulation Parameters

Parameter	**Value**
Operational Area	0.5 square mile
Min Tx-Tx separation	10 m
Tx-Rx separation	$Uniform(10m, 100m)$
Frequency shift (Δf)	1 MHz
Power margin threshold	3 dB
Number of trials	100
Python version	3.8
Machine configuration	Intel i7-4790 (3.60 GHz) Cores: 8, Memory: 15 GB

A. Simulation Results

1) Spectrum usage: We evaluate the spectrum usage of Algorithm 1 by considering the number of frequency channels used. As shown in Fig. 2, for 100 trials, the ***maximum*** number of channels required to configure 10 links is 5 as compared to 17 channels required to configure 100 links. The ***mode*** number of channels required for 10, 50 and 100 links are 3, 8 and 13, respectively. We also observe that, to support a large number of links (100 in our case), we require only a few channels (17 channels max) and this is mainly due to the Tx power adjustment, as shown in Table III. We limit the Tx power of new transmitters based on the power margin threshold and the power margin obtained from the CT. If a CT indicates that the Tx power of a transmitter will lead to compatibility with all previous receivers if reduced by an amount that does not exceed the value indicated by the power margin threshold, then the adjustment is applied. Otherwise, the transmitter moves to a different frequency/channel. The average number of Tx power adjustments for 10 and 100 links over 100 trials is found to be 1.09 and 69.91, respectively, highlighting the importance of Tx power adjustments on reducing spectrum usage. For scenarios with a large number of links, the Tx power adjustment step can (occasionally) lead to a transmitter not being able to reach its intended receiver. This forces the use of a different frequency

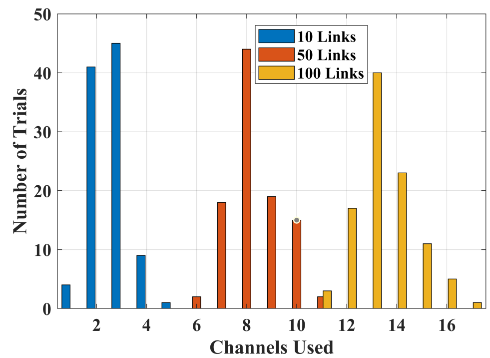

Fig. 2: Histogram showing the number of channels used by Algorithm 1 to deconflict networks of different sizes.

channel for the Tx/Rx pair and the need to perform CTs again. The average non-reachable link events for 100 links over 100 trials is found to be 5.86, requiring higher computation time to deconflict the spectrum as described in section V-A2.

TABLE III: Performance counters of Algorithm 1 averaged over 100 trials for different network sizes

Links	**10**	**20**	**50**	**80**	**100**
Avg. # of power adjustments	1.09	6.93	29.46	52.74	69.91
Avg. # of non-reachable events	0.04	0.29	1.9	3.65	5.86

TABLE IV: Presence of aggregate interference averaged over 100 trials for different network sizes

Links	**10**	**20**	**50**	**80**	**100**
Baseline	0.13	0.64	6.63	20.94	32.99
Algorithm 1	0.05	0.81	7.18	19.36	29.89

We also compare the spectrum usage of Algorithm 1 and the baseline algorithm considering 100 links. In Fig. 3, when looking at the ***mode/max*** values, higher number of channels are required for the baseline case as compared to our proposed scheme, since the baseline algorithm just operates on assigning frequencies without adapting Tx power levels. The other important metric in the evaluation is the presence of aggregate interference in the system. We defined a counter for aggregate interference events that is incremented only when a new receiver is compatible with all existing transmitters on a one-to-one basis, but not when taking into account the interference caused by all existing transmitters. Table IV provides the average number of times (cases) that aggregate interference effects led to an incompatibility decision in 100 runs/trials. In each of those cases, the device would need to move to a different frequency to be protected from aggregate interference effects. The results obtained indicate that as the number of devices grows, the effects of aggregate interference and adjacent channel power leakage are well captured with the use of SCMs. A higher number of aggregate interference events is observed for the baseline algorithm as compared to Algorithm 1, due to the presence of a large number of channels being used at full power. Moreover, the aggregate interference highly depends on the Tx/Rx location coordinates and the channels being used. Further, Algorithm 1 without power margin threshold (no PMT) when compared against the baseline algorithm, achieves a better spectral efficiency (see Fig. 3) due to the more flexible power assignment and fewer number of aggregate interference cases.

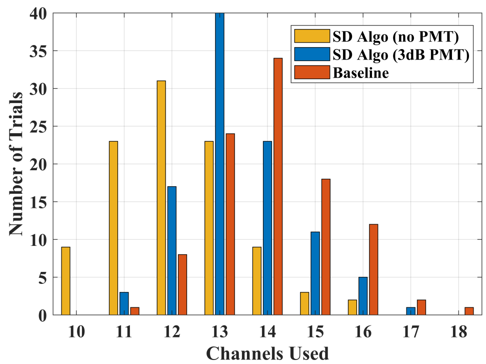

Fig. 3: Histogram showing the number of channels used among SD algorithm variants (100 links & 100 trials).

2) Computation time: We evaluate the time required to deconflict the spectrum use, i.e., the time to determine compatible parameters for every Tx/Rx pair in the operational area. The computation time does not include: (i) pauses between new link pair instances (recall that pairs join the system sequentially); (ii) time to turn on the RF devices, which depends on the radios being used; (iii) SCM transmission times, which usually take a few milliseconds. Figure 4 shows the mean computation time for networks with different numbers of Tx/Rx pairs. For each simulation setup, 100 trials/runs are executed. We observe that to configure a single new link (Tx/Rx pair) in a scenario composed of 20 pre-existing links Algorithm 1 with a 3dB PMT takes (on average) 0.37 seconds as compared to the 3.25 seconds required in a scenario with 100 pre-existing link-pairs. The increase in computation time with the increase in the total number of Tx/Rx pairs is expected and it is mainly due to the larger number of CTs that need to be performed. To setup a single new link in a scenario that already has 100 operational link-pairs, the baseline algorithm takes (on average) 3.51 seconds. The increase in computation time with the increase in the number of links for the baseline algorithm is due to the large number of CTs needed to perform deconfliction over a larger number of channels to minimize aggregate interference. This is in contrast to the Algorithm 1 no PMT case where the number of channels over which to perform CTs is lower. Overall, the computation times can be significantly reduced by using more powerful CPUs and with additional algorithm optimizations.

3) SD algorithm enhancement: To further evaluate and enhance the performance of the spectrum deconfliction achieved by Algorithm 1, we introduce a distance parameter (D), where we only perform CTs with the devices that are within a distance D from each other, rather than with all existing devices. When setting D=100m or D=300m, the computation time is

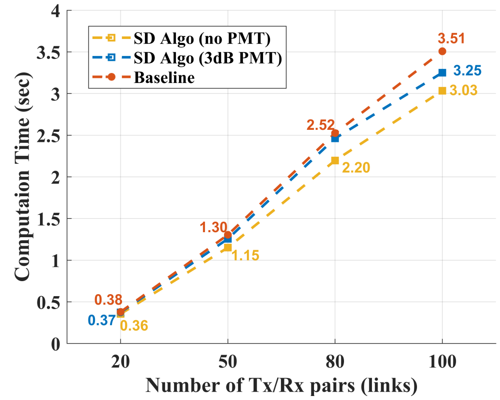

Fig. 4: Average time required per link among SD algorithm variants and the Baseline algorithm to deconflict spectrum use.

significantly reduced as compared to the exhaustive case. As an example, having 100 links, the average computation time for D=100m and D=300m is 0.151s and 0.881s, respectively as compared to 3.25s required for the non-distance constrained version of Algorithm 1 (see Table V). For D=500m, the spectrum usage and the impact of aggregate interference is similar to that of the exhaustive solution (SD Algorithm, see Fig. 5), implying that for up to 500m, the aggregate interference from existing devices is impacting the new device and is well captured with the help of SCMs. In some cases, the use of the distance parameter led to compatibility errors and we compute this error with respect to the exhaustive case where the evaluation of compatibility is done against all existing devices. The results are shown in Table V. We see that the compatibility error decreases with the increase in D, since more devices will be considered in CT computations allowing to accurately capture the impact of aggregate interference at each receiver. Also, a high compatibility error is observed for D=100m. Intuitively, the error drops significantly beyond that distance mainly because each transmitter's coverage radius is roughly 100m. The results indicate that based on the sensitivity of the new device/receiver that is trying to operate in the area, and assuming a constant maximum level for the transmit power for all transmitters, an appropriate D parameter should be selected to reduce the number of compatibility computations and minimize the probability of error from such reduction.

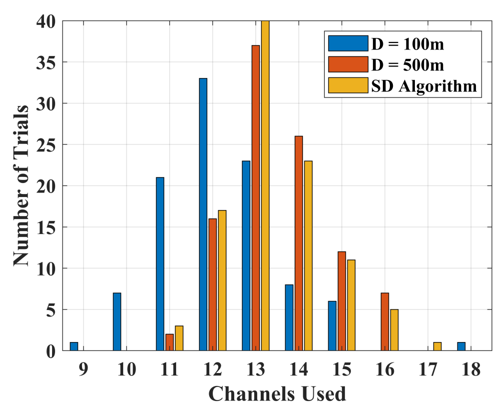

Fig. 5: Histogram showing the channel usage - D constrained vs. non-constrained Algorithm 1 (100 links & 100 trials).

TABLE V: Global compatibility error (%) and average computation time per link (in seconds) due to the use of the distance (D) parameter for Algorithm 1, averaged over 30 random trials in networks of different sizes.

	20 Links		**50 Links**		**80 Links**		**100 Links**	
	Error (%)	**Time (sec)**	**Error (%)**	**Time (sec)**	**Error (%)**	**Time (sec)**	**Error (%)**	**Time (sec)**
D = 100m	13.5	0.022	22.33	0.065	24.5	0.109	23.4	0.151
D = 200m	2.0	0.053	2.0	0.175	0.75	0.341	0.933	0.467
D = 300m	1.66	0.103	0.133	0.321	0.166	0.621	0.133	0.881
D = 500m	0	0.205	0	0.662	0.08	1.317	0	1.8

4) Channel separation: Finally, we evaluate the spectrum usage of Algorithm 1 considering a wider channel separation where every new channel has its center frequency 2 MHz away from the last channel used. As shown in Fig. 6, for 100 trials, we observe that, using 2 MHz separation results in a lower number of used channels, but at the cost of wider total spectrum occupancy as compared to channels having 1 MHz separation (see Fig. 2). Also, lower computation times (2.39s, 100 links) are observed mainly due to channels being well apart resulting in lower adjacent channel (aggregate) interference and fewer power adjustment events with non-reachable link events, thus allowing the devices to find optimal parameters faster with a lower number of compatibility tests.

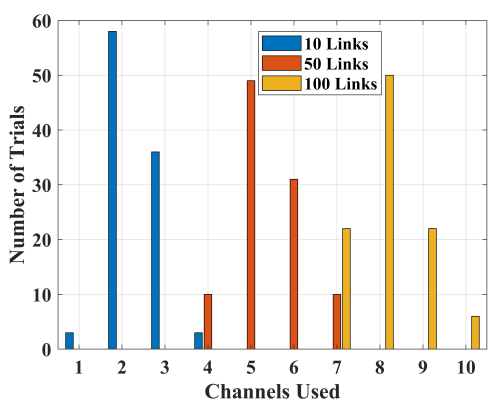

Fig. 6: Histogram showing the number of channels used by Algorithm 1 to deconflict using 2 MHz channel separation.

VI. Conclusion and Future Work

This paper presented a novel mechanism for performing spectrum coordination using SCMs which offer a standardized means to capture the spectral, temporal, and spatial characteristics of spectrum use of RF devices and systems. The proposed algorithm dynamically adjusts the transmission parameters, ensuring aggregate compatibility among all existing RF devices. The algorithm was evaluated in terms of computation time, efficiency of spectrum allocation, and number of device reconfigurations using a custom platform that simulates dynamic and dense communication environments. The simulation results in this paper and the experimental validation in [10] demonstrate the feasibility of our SCM-based spectrum deconfliction technique in performing fine grained spectrum assignments at scale.

In future work, we will consider networks with mmWave nodes using phased array antennas and develop enhanced SCM-based DSA algorithms that take into account antenna directionality and develop machine learning-based algorithms to enable efficient SCM based spectrum access schemes.

VII. Acknowledgements

This work was supported in part by NSF grants CNS-2148128, CNS-1827923, OAC-2029295, AST-2232455, AST-2232456, AST-2232459, EEC-2133516

References

[1] W. S. H. M. W. Ahmad, N. A. M. Radzi, F. Samidi, A. Ismail, F. Abdullah, M. Z. Jamaludin, and M. Zakaria, "5G technology: Towards dynamic spectrum sharing using cognitive radio networks," *IEEE Access*, 2020.

[2] P. Karimi, W. Lehr, I. Seskar, and D. Raychaudhuri, "SMAP : A scalable and distributed architecture for dynamic spectrum management," in *Proc. of IEEE DySPAN*, 2018.

[3] F. Paisana, Z. Khan, J. Lehtomäki, L. A. DaSilva, and R. Vuohtoniemi, "Exploring radio environment map architectures for spectrum sharing in the radar bands," in *Proc. of IEEE ICT*, 2016.

[4] H. B. Yilmaz, T. Tugcu, F. Alagöz, and S. Bayhan, "Radio environment map as enabler for practical cognitive radio networks," *IEEE Communications Magazine*, 2013.

[5] J. A. Stine and C. E. C. Bastidas, "Enabling spectrum sharing via spectrum consumption models," *IEEE Journal on Selected Areas in Communications*, 2015.

[6] H. Harada, Y. Alemseged, S. Filin, M. Riegel, M. Gundlach, O. Holland, B. Bochow, M. Ariyoshi, and L. Grande, "IEEE dynamic spectrum access networks standards committee," *IEEE Communications Magazine*, 2013.

[7] C. E. C. Bastidas, J. A. Stine, A. Rennier, M. Sherman, A. Lackpour, M. M. Kokar, and R. Schrage, "IEEE 1900.5.2: Standard method for modeling spectrum consumption: Introduction and use cases," *IEEE Communications Standards Magazine*, 2018.

[8] S. Haykin, D. J. Thomson, and J. H. Reed, "Spectrum sensing for cognitive radio," *Proceedings of the IEEE*, 2009.

[9] N. Muchandi and R. Khanai, "Cognitive radio spectrum sensing: A survey," in *Proc. of IEEE ICEEOT*, 2016.

[10] D. Stojadinovic, P. Netalkar, C. E. Caicedo, I. Kadota, G. Zussman, I. Seskar, and D. Raychaudhuri, "A spectrum consumption model-based framework for DSA experimentation on the cosmos testbed," in *Proc. of ACM WiNTECH*, 2021.

[11] D. Raychaudhuri, I. Seskar, G. Zussman, T. Korakis, D. Kilper, T. Chen, J. Kolodziejski, M. Sherman, Z. Kostic, X. Gu *et al.*, "Challenge: COSMOS: A city-scale programmable testbed for experimentation with advanced wireless," in *Proc. of ACM MobiCom*, 2020.

[12] IEEE, "IEEE 1900.5.2-2017 - IEEE standard for method for modeling spectrum consumption," 2017.

[13] D. Altner, S. Schmitz, J. A. Stine, and J. Snider, "Determining aggregate compatibility using dynamic spectrum consumption models via global optimization," in *Optimization Online*, 2016.

[14] "Spectrum consumption model builder and analysis tool (SCMBAT)," https://github.com/ccaicedo/SCMBAT, 2022.